

Ventilation Distribution Studies Comparing Technegas and “Gallgas” Using $^{68}\text{GaCl}_3$ as the Label

João Batista Borges^{1,2}, Irina Velikyan^{3,4}, Bengt Långström⁴, Jens Sörensen⁵, Johan Ulin³, Enn Maripuu⁶, Mattias Sandström⁶, Charles Widström⁶, and Göran Hedenstierna¹

¹Department of Medical Sciences, Clinical Physiology, Uppsala University, Uppsala, Sweden; ²Pulmonary Division, Cardio-Pulmonary Department, Hospital das Clínicas, University of São Paulo, São Paulo, Brazil; ³Uppsala Applied Sciences Laboratory, GE Healthcare, Uppsala, Sweden; ⁴Department of Biochemistry and Organic Chemistry, Uppsala University, Uppsala, Sweden; ⁵Department of Nuclear Medicine, Uppsala University Hospital, Uppsala, Sweden; and ⁶Department of Medical Physics, Uppsala University Hospital, Uppsala, Sweden

Ventilation distribution can be assessed by SPECT with Technegas. This study was undertaken in piglets with different degrees of ventilation inhomogeneity to compare PET using ^{68}Ga -labeled pseudogas or “Gallgas” with Technegas. **Methods:** Twelve piglets were studied in 3 groups: control, lobar obstruction, and diffuse airway obstruction. Two more piglets were assessed for lung volume (functional residual capacity). **Results:** In controls, SPECT and PET images showed an even distribution of radioactivity. With lobar obstruction, the absence of ventilation of the obstructed lobe was visible with both techniques. In diffuse airway obstruction, SPECT images showed an even distribution of radioactivity, and PET images showed more varied radioactivity over the lung. **Conclusion:** PET provides detailed ventilation distribution images and a better appreciation of ventilation heterogeneity. Gallgas with PET is a promising new diagnostic tool for the assessment of ventilation distribution.

Key Words: ventilation; Technegas; SPECT; ^{68}Ga -pseudogas; PET

J Nucl Med 2011; 52:206–209

DOI: 10.2967/jnumed.110.083881

Ventilation distribution is regularly studied before lung resection and is also part of the diagnosis of pulmonary emboli (1).

The standard technique for assessing ventilation distribution by γ -camera is the use of Technegas (Vita Medical Ltd.). Small carbon particles (0.2–0.4 μm) behave as a pseudogas and are distributed within the airway tree down to the alveoli during inspiration. The subject lies under a γ -camera, and a 2-dimensional planar view or a 3-dimensional SPECT scan is acquired.

PET offers better resolution than SPECT (2), and if repeated measurements are required, the shorter half-lives of positron-emitting isotopes may allow more rapid investigations than with γ -emitting isotopes.

A prerequisite is that the ventilation marker be easy to administer. The equipment for producing Technegas might also be used to prepare a pseudogas for which the carbon particles are labeled with positron-emitting ^{68}Ga as GaCl_3 . ^{68}Ga is readily available from a long-shelf-life $^{68}\text{Ge}/^{68}\text{Ga}$ generator, and it decays by 89% through positron emission.

This study was undertaken in a porcine model of different degrees of ventilation inhomogeneity to compare PET using ^{68}Ga -labeled pseudogas (Gallgas) with standard SPECT using Technegas.

MATERIALS AND METHODS

Preparation of Gallgas

^{68}Ga (half-life of 68 min, decay by positron emission [89%], and electron capture [11%]) was available from a $^{68}\text{Ge}/^{68}\text{Ga}$ generator system in which ^{68}Ge (half-life, 270.8 d) was attached to a column of an inorganic matrix using titanium dioxide. The nominal ^{68}Ge radioactivity loaded onto the generator column was 1,850 MBq. The specified shelf-life of the generator was 2–3 y. The ^{68}Ga was eluted with 6 mL of 0.1 M hydrochloric acid. The whole volume of the eluate was preconcentrated on an anion-exchange cartridge to decrease the volume of the generator eluate (from 6 mL to 200 μL) (3).

Gallgas was prepared on the commercially available Technegas Plus Generator (Vita Medical Ltd.). The standard procedure was used, including the prewetting of the crucible with ethanol before the application of the $^{68}\text{GaCl}_3$ solution. The preconcentrated ^{68}Ga solution (100–140 μL ; 50–100 MBq) was applied to the graphite crucible and evaporated in the furnace at 50°C–70°C. ^{68}Ga was then encapsulated by carbon composites. Gallium metal was covered by layers of graphite sheets that isolated the metal from the external environment (performed at 2,500°C–2,700°C for 15–20 s). The imaging agent was used for the experiments via inhalation within 10 min to avoid aggregation of the particles.

Imaging Techniques

The animals were studied supine, first on a CT-equipped γ -camera using inhalation of Technegas and then on a PET/CT camera using inhalation of Gallgas. The radioactivity inhaled by

Received Oct. 4, 2010; revision accepted Nov. 3, 2010.

For correspondence or reprints contact: Göran Hedenstierna, Department of Medical Sciences, Clinical Physiology, Uppsala University Hospital, 751 85, Uppsala, Sweden.

E-mail: goran.hedenstierna@medsci.uu.se

COPYRIGHT © 2011 by the Society of Nuclear Medicine, Inc.

TABLE 1
Physiologic Data

Group	Compliance	Resistance	PaO ₂ /F _I O ₂
Healthy-lung control	22.5 ± 3.6	9.2 ± 2.6	429 ± 46
Lobar obstruction	18.1 ± 1.8	11.9 ± 1.6	258 ± 45*
Diffuse obstruction	21.1 ± 4.6	15.3 ± 6.4†	309 ± 125†

*Significant difference between lobar obstruction and healthy-lung control groups ($P < 0.05$).

†Significant difference between diffuse obstruction and healthy-lung control groups ($P < 0.05$).

Data were not significantly different between SPECT and PET measurements and have, therefore, been pooled. Data are expressed as mean ± SD.

the piglets was 30 and 5–10 MBq, respectively, for ^{99m}Tc and ⁶⁸Ga. A vacuum mattress was used to keep the piglet in the same position during the experiments and when the animal was moved between the cameras.

SPECT Acquisition

SPECT was performed on a dual-head γ -camera (Infinia; GE Healthcare) equipped with all-purpose, low-energy collimators. The SPECT images were acquired with a low-energy general-purpose collimator in 60 projections (30 per head) stored in a 128 matrix. The acquisition time was 30 s per projection. Low-resolution CT (2.5 mA, 140 kV) was performed covering the same volume as the SPECT acquisition to evaluate lung borders and enable attenuation correction. The overall acquisition time was 25 min. Data were then reconstructed on a Xeleris workstation using a reconstruction technique with 4 iterations, 8 subsets, and a Hann 3-dimensional postreconstruction filter.

PET Acquisition

PET was performed on a Discovery VCT scanner (GE Healthcare). The acquisition mode used a 3-dimensional imaging technique, a scan time of 3 min per bed position, 128 × 128 pixels, and a 70 cm field of view. The VUE Point HD iterative reconstruction algorithm (GE Healthcare) was used to reconstruct images with 2 iterations and 28 subsets. The z-axis filter was a standard box car (1-4-1), and the postprocessing filter was set to 6.00 mm (in full width at half maximum). Images from the CT study were attenuation-corrected 120 kV; 30–80 mA; smart mA and auto mA (GE Healthcare); and rotation time, 0.5 s).

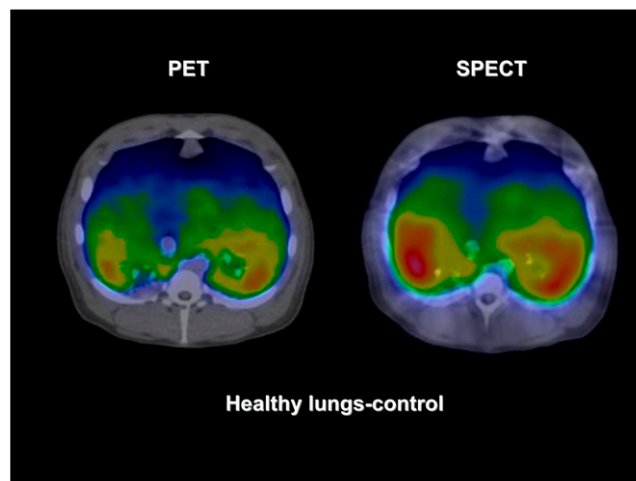


FIGURE 1. PET/CT (⁶⁸Ga) and SPECT/CT (^{99m}Tc) images of lung ventilation in healthy piglet. Ventilation distribution on PET and SPECT images is similar.

Analysis Techniques: Distribution Volume for Pseudogas

The distribution volume for the pseudogas when labeled either with ⁶⁸Ga or with ^{99m}Tc was calculated from the SPECT and PET images as the sum of all voxels multiplied by the individual voxel volume that contained radioactivity of ⁶⁸Ga or ^{99m}Tc inside the lung. Lungs were delineated by creating a lung mask from the CT image.

The variation in tracer gas radioactivity, reflecting any inhomogeneity in the distribution of the gas, was calculated by applying statistical modeling.

Protocol. Fourteen piglets were mechanically ventilated under a continuous administration of ketamine, fentanyl, and pancuronium. Physiologic data were intermittently acquired.

Twelve animals were allocated to the following 3 groups, with 4 piglets in each group: healthy-lung control, normal ventilation distribution; lobar obstruction, a balloon catheter occluding a lower main bronchus; and diffuse obstruction, a continuous methacholine (4,5) infusion adjusted to cause an increase in respiratory resistance by 50%.

The pseudogas was administered to the lungs using a 2-L syringe, 0.5 L of gas was aspirated from the generator box, and 0.5 L was inflated into the lungs. Then the deflation and inflation process was repeated 4 times.

TABLE 2
Distribution Volume, FRC, and Heterogeneity Index

Group	Distribution volume		FRC (n = 2)	R ² *	
	SPECT (n = 4)	PET (n = 4)		SPECT (n = 4)	PET (n = 4)
Healthy-lung control	1,023 ± 126	989 ± 251	713 ± 100	0.72 ± 0.14	0.72 ± 0.1
Lobar obstruction	919 ± 84	771 ± 101		0.75 ± 0.07	0.67 ± 0.03
Diffuse obstruction	1,064 ± 70	880 ± 96†	676 ± 97	0.8 ± 0.01	0.56 ± 0.19

*Significant difference between SPECT and PET ($P < 0.05$).

†Significant difference between SPECT and PET ($P < 0.05$).

R² = coefficient of determination (heterogeneity index).

Data are expressed as mean ± SD.

In addition, 2 piglets were studied using similar anesthesia during baseline and infusion of methacholine, with measurement of their end-expiratory lung volume (functional residual capacity [FRC]) by multiple-breath nitrogen washout (6).

Statistics

PET and SPECT counts were log-transformed in a transversal slice (the one with the largest lung area) to enable a regression analysis of the heterogeneity of the ventilation distribution. For each piglet, the transformed PET and SPECT counts were related to 2-dimensional coordinates (i.e., x , y from that slice) in a regression model using a quadratic function of the coordinates. The quadratic function was fitted for the 2 lungs combined, delineated by the created lung masks from the CT images.

The difference between the coefficients of determination (R^2) from the 2 models (the SPECT and PET) was calculated for each piglet, and a Wilcoxon matched-pairs signed-rank test was performed to test the null hypothesis of equal R^2 .

For the other physiologic variables, we used repeated-measures ANOVA for comparisons during the protocol. Significance was defined as a P level (bicaudal) of less than 0.05.

RESULTS

Physiology

Compared with the control animals, methacholine infusion increased respiratory resistance by 67% ($P < 0.05$) and caused a fall in the ratio of partial pressure of arterial O_2 (PaO_2) to the fraction of inspired O_2 ($F_I O_2$) ($P < 0.05$), as is consistent with diffuse bronchial obstruction. Lobar obstruction caused a significant drop in $PaO_2/F_I O_2$ ($P < 0.05$), reasonably explained by continuing perfusion of the nonventilated lobe. However, there was no significant difference in resistance, or in respiratory compliance or arterial oxygenation, between measurements done during the SPECT and PET investigations (Table 1).

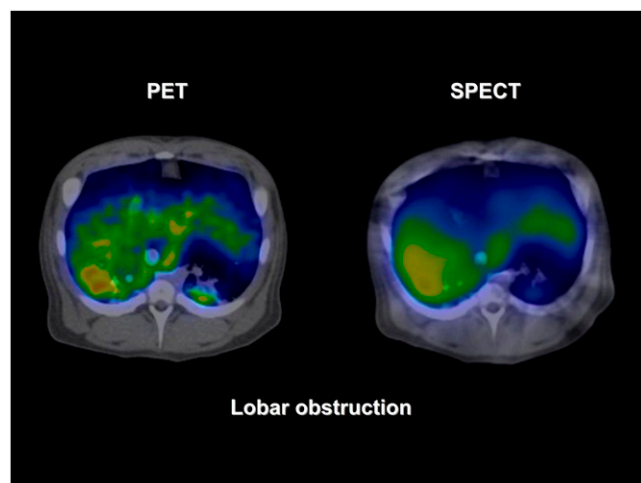


FIGURE 2. PET/CT (^{68}Ga) and SPECT/CT ($^{99\text{m}}\text{Tc}$) images of lung ventilation during lower lobar obstruction. Ability of images to detect absence of ventilation corresponding to lower lobe is similar. Ventilation distribution on PET image varies more than that on SPECT image, perhaps suggesting diffuse bronchial constriction as consequence of lobar obstruction, which is not detected with SPECT.

For the healthy-lung control group, SPECT and PET images showed an even distribution of activity (Fig. 1), reflecting homogeneous ventilation distribution. The distribution volumes for Technegas and Gallgas were similar (Table 2). For the lobar obstruction group, the absence of ventilation of the lower lobe was clearly visible on both SPECT and PET images (Fig. 2). For the diffuse obstruction group, distribution volumes for ^{68}Ga and $^{99\text{m}}\text{Tc}$ differed considerably, with the volume for ^{68}Ga being lower than that for $^{99\text{m}}\text{Tc}$ ($P < 0.05$; Table 2).

Despite an expected inhomogeneity of ventilation distribution during methacholine infusion, the SPECT image showed a smooth and even distribution of activity (Fig. 3). The PET image showed a more varied activity over the lung field, indicating inhomogeneity of the ventilation.

Variation in Tracer Gas Activity for SPECT and PET

The difference between the R^2 values from the SPECT and PET models was calculated for each piglet and resulted in significantly less variability in tracer gas activity for SPECT than for PET ($P < 0.05$; Table 2).

FRC During Methacholine Infusion

The smaller distribution volume for ^{68}Ga than for $^{99\text{m}}\text{Tc}$ prompted the additional experiments on FRC. These experiments showed a decrease in FRC during methacholine infusion (Table 2).

DISCUSSION

This study showed that measurement of ventilation distribution with the PET tracer ^{68}Ga (Gallgas) resulted in more detailed images than with SPECT using $^{99\text{m}}\text{Tc}$ (Technegas).

We obtained technically good results in all 12 piglets. SPECT and PET images were similar in the healthy controls, with even distributions of ventilation. Bronchial

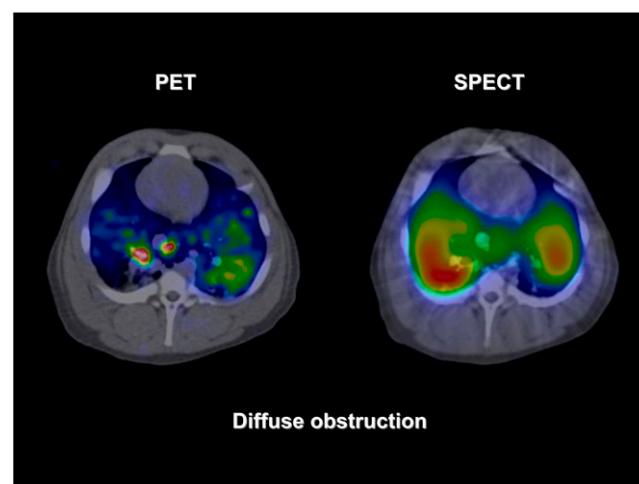


FIGURE 3. PET/CT (^{68}Ga) and SPECT/CT ($^{99\text{m}}\text{Tc}$) images of lung ventilation during methacholine infusion, which causes diffuse airway obstruction. Ventilation distribution on PET image varies more than that on SPECT image. This larger variation was also supported by statistical analysis shown in Figure 4.

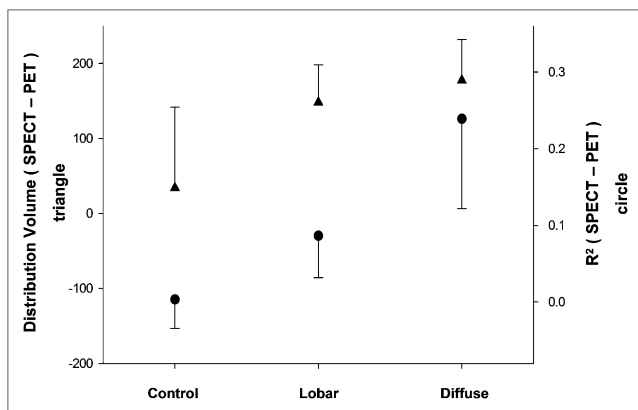


FIGURE 4. Difference in distribution volumes between SPECT (^{99m}Tc) and PET (^{68}Ga) (▲) images and difference between R^2 for distribution volumes (●). R^2 corresponds to residual SD—that is, scatter of individual observations along regression line. Higher R^2 indicates closer fit to regression line and thus less variation in distribution of tracer gas. Parallel shift of difference in distribution volume and R^2 when going from control to lobar obstruction to diffuse obstruction shows that decreased distribution volume for PET (^{68}Ga), compared with distribution volume for SPECT (^{99m}Tc), occurs simultaneously with increased heterogeneity of dispersion of ^{68}Ga . Data are expressed as mean \pm SEM.

occlusion eliminated ventilation to the lower lobe (right or left lung), with good visualization with both techniques. However, distribution of the tracer in the ventilated lung tissue was more detailed on the PET image.

Diffuse airway obstruction by methacholine infusion showed a much larger distinction between poorly and well-ventilated regions on the PET image than on the SPECT image. This difference may be related to the lower spatial resolution of SPECT. This difference could also be visualized when PET methacholine images were smoothed by a Butterworth filter (cutoff, 0.7 cycles/cm; order, 2). The full width at half maximum for PET was similar to that for SPECT (15.5 and 15.6 mm, respectively). After the smoothing, the PET images resembled the SPECT images—that is, the PET images no longer showed the large variation in ventilation distribution caused by the methacholine.

The smaller distribution volume for the ^{68}Ga than for the ^{99m}Tc caused some concern that ^{68}Ga did not reach the lung periphery as well as did the ^{99m}Tc . However, the recording of FRC in the 2 additional piglets showed a decrease in their FRC on methacholine infusion, more in line with the drop in Gallgas distribution volume than the increase seen with Technegas. Therefore, reduced FRC suggests bronchial obstruction and airway closure by the methacholine (7–9) that limits the spread of ^{68}Ga (and ^{99m}Tc) to all lung units. The larger distribution volume for ^{99m}Tc will then be an artifact, related to the poorer resolution of the ^{99m}Tc activity. With poorer resolution, there will be less ability to distinguish between well- and poorly ventilated lung regions if these regions are near one another.

Further support for this interpretation comes from the correlation between the heterogeneity index (R^2) and dis-

tribution volume—the smaller the R^2 , the smaller the distribution volume, as shown in Table 2 and Figure 4.

Our study has limitations, such as the small number of animals investigated. The 2 techniques were not compared at the same time because we had to use 2 different cameras. Therefore, lung ventilation may not have been identical at the 2 times of imaging. To overcome this, we performed a procedure to homogenize the lung history before and between each acquisition of PET and SPECT images.

To support the homogenization of lung history, respiratory mechanics and oxygenation were similar during SPECT and PET in all 3 experiments. Lung ventilation distribution measurements with PET have methodologic limitations. Partial-volume averaging and spillover effects affect radioactivity quantification with PET, mainly in the peripheral parts of the lungs.

CONCLUSION

PET provided detailed ventilation distribution images and a better appreciation of heterogeneity of the airway response to a bronchoconstrictive challenge than did SPECT. Gallgas and PET is a promising new diagnostic tool for the assessment of ventilation distribution.

ACKNOWLEDGMENTS

We thank Agneta Roneus, Karin Fagerbrink, Pia Bostrom, Anna Eriksson, and Aseel Sherif for their help with the study. This study was supported by grants from institutional funds from Uppsala University and Coordenação de Aperfeiçoamento de Pessoal de Nível Superior (CAPES)—Ministry of Education, Brazil, and by GE Healthcare. Consumables for the generation of Technegas and carbon boats for Gallgas were provided by Hans-Olof Sandberg, Medica-Nordic AB.

REFERENCES

- Zophel K, Bacher-Stier C, Pinkert J, Kropp J. Ventilation/perfusion lung scintigraphy: what is still needed? A review considering technetium-99m-labeled macroaggregates of albumin. *Ann Nucl Med*. 2009;23:1–16.
- Spanoudaki VC, Ziegler SI. PET & SPECT instrumentation. *Handb Exp Pharmacol*. 2008;(185 Pt 1):53–74.
- Velikyan I, Beyer GJ, Langstrom B. Microwave-supported preparation of ^{68}Ga bioconjugates with high specific radioactivity. *Bioconjug Chem*. 2004;15:554–560.
- Leff AR, Munoz NM. Cholinergic and alpha adrenergic augmentation of histamine-induced contraction of canine airway smooth muscle. *J Pharmacol Exp Ther*. 1981;218:582–587.
- Leff AR, Munoz NM, Alderman B. Measurement of airway response by isometric and nonisometric techniques in situ. *J Appl Physiol*. 1982;52:1363–1367.
- Hedenstierna G, Strandberg A, Brismar B, Lundquist H, Svensson L, Tokics L. Functional residual capacity, thoracoabdominal dimensions, and central blood volume during general anesthesia with muscle paralysis and mechanical ventilation. *Anesthesiology*. 1985;62:247–254.
- Amirav I, Kramer SS, Grunstein MM. Methacholine-induced temporal changes in airway geometry and lung density by CT. *Chest*. 2001;119:1878–1885.
- Amirav I, Kramer SS, Grunstein MM, Hoffman EA. Assessment of methacholine-induced airway constriction by ultrafast high-resolution computed tomography. *J Appl Physiol*. 1993;75:2239–2250.
- Herold CJ, Brown RH, Mitzner W, Links JM, Hirshman CA, Zerhouni EA. Assessment of pulmonary airway reactivity with high-resolution CT. *Radiology*. 1991;181:369–374.



The Journal of
NUCLEAR MEDICINE

Ventilation Distribution Studies Comparing Technegas and "Gallgas" Using $^{68}\text{GaCl}_3$ as the Label

João Batista Borges, Irina Velikyan, Bengt Långström, Jens Sørensen, Johan Ulin, Enn Maripuu, Mattias Sandström, Charles Widström and Göran Hedenstierna

J Nucl Med. 2011;52:206-209.

Published online: January 13, 2011.

Doi: 10.2967/jnumed.110.083881

This article and updated information are available at:

<http://jnm.snmjournals.org/content/52/2/206>

Information about reproducing figures, tables, or other portions of this article can be found online at:

<http://jnm.snmjournals.org/site/misc/permission.xhtml>

Information about subscriptions to JNM can be found at:

<http://jnm.snmjournals.org/site/subscriptions/online.xhtml>

The Journal of Nuclear Medicine is published monthly.
SNMMI | Society of Nuclear Medicine and Molecular Imaging
1850 Samuel Morse Drive, Reston, VA 20190.
(Print ISSN: 0161-5505, Online ISSN: 2159-662X)

© Copyright 2011 SNMMI; all rights reserved.

The logo for the Society of Nuclear Medicine and Molecular Imaging (SNMMI) features the letters 'S', 'N', 'M', and 'I' in a stylized, overlapping arrangement. The 'S' and 'N' are in the top row, and the 'M' and 'I' are in the bottom row. The letters are white with a red outline, set against a red square background.
SOCIETY OF
NUCLEAR MEDICINE
AND MOLECULAR IMAGING